Journal of Solid Mechanics Vol. 11, No. 2 (2019) pp. 409-424
DOI: 10.22034/JSM.2019.665367

# Buckling and Thermomechanical Vibration Analysis of a Cylindrical Sandwich Panel with an Elastic Core Using Generalized Differential Quadrature Method

A.R. Pourmoayed [1,*], K. Malekzadeh [2], M. Shahravi [2], H. Safarpour [3]

[1]*Department of Mechanical Engineering, Khatamul-Anbiya Air Defense University, Tehran, Iran*
[2]*Faculty of Structural Analysis and Simulation Centre, MalekAshtar University,Tehran, Iran*
[3]*Department of Mechanics, Imam Khomeini International University, Qazvin, Iran*

Received 14 March 2019; accepted 10 May 2019

**ABSTRACT**

In this paper, the vibrational and buckling analysis of a cylindrical sandwich panel with an elastic core under thermo-mechanical loadings is investigated. The modeled cylindrical sandwich panel as well as its equations of motions and boundary conditions is derived by Hamilton's principle and the first-order shear deformation theory (FSDT). For the first time in the present study, various boundary conditions is considered in the cylindrical sandwich panel with an elastic core. In order to obtain the temperature distribution in the cylindrical sandwich panel in the absence of a heat-generation source, temperature distribution is obtained by solving the steady-state heat-transfer equation. The accuracy of the presented model is verified using previous studies and the results obtained by the Navier analytical method. The novelty of the present study is considering thermo-mechanical loadings as well as satisfying various boundary conditions. The generalized differential quadrature method (GDQM) is applied to discretize the equations of motion. Then, some factors such as the influence of length-to-radius ratio, circumferential wave numbers, thermal loadings, and boundary conditions are examined on the dynamic and static behavior of the cylindrical sandwich panel.



**Keywords :** Heat-transfer equation; Buckling and vibration behavior; GDQM; Cylindrical sandwich panel; Various boundary conditions.

## 1 INTRODUCTION

IN recent years, the use of sandwich structures in civil, transportation, naval, and aerospace macro-design components have increased because of their outstanding bending rigidity, low specific weight, superior isolating qualities, excellent vibration characteristics, and good fatigue properties. Sandwich structures are constructed of three layers. They are usually composed of two metallic or composite laminated materials: face sheets and a foam core or a low-strength honeycomb core. An important design consideration for such shell structures is their buckling capacity under various pressure loadings [1]. Moreover, temperature variations are one of the most important factors

*Corresponding author. Tel.: +98 21 33228535; Fax: +98 21 33228503.
*E-mail address: pourmoayed@mut.ac.ir* (A.R. Pourmoayed).

for stress fields in structures such as multilayered composite plates and shells that cause their failure. Advanced composite materials consist of a number of properties including high specific strength and stiffness and nearly zero coefficient of thermal expansion in fiber orientation. Because of these implications, the effects of high temperature and mechanical loadings have to be considered in the design process of such structures [2, 3]. Therefore, the behavior of high-temperature composite plates and shells has received increasing attention. Different approaches may be used for modeling sandwich panels. Many shell studies incorporate classical shell theories which are based on Kirchhoff–Love's hypothesis (see, for example, Refs. [4, 5]. Some studies based on 3D elasticity theory have been conducted on the vibration analysis of isotropic and composite cylindrical shells [6, 7]. In such research works, Ritz method, finite-element method, and series solutions were employed. Unlike the equivalent single-layer theories (ESL), the layerwise theory assumes separate displacement field expansions within each subdivision. Moreover, the layerwise theory provides a kinematically correct representation of the strain field in discrete layers. Eslami and Shariyat [8] buckling of thin cylindrical shells under different mechanical loading conditions used Donnell's nonlinear theory of shells are studied. Also, in Eslami et al. [9], the thermoelastic buckling of thin cylindrical shells under a number of practical thermal loadings were obtained based on Donnell and improved Donnell equations. The thermal buckling of composite cylindrical shells subjected to a uniform temperature rise was examined by Radhamohan and Enkataramana [10]. Alibeiglo [11] presented thermo-mechanical analysis of a simply supported sandwich cylindrical panel using an analytically method. Alibeiglo in this work studied the effects of key parameters on critical temperature and critical load of the sandwich panel. Based on the finite-element method, the buckling of laminated composite cylindrical and conical shells under thermal load was studied by Thangaratnam et al. [12]. Bert [13] considered the effect of temperature on the buckling and postbuckling behavior of reinforced and unstiffened composite plates and cylindrical shells. In this paper, to obtain the critical buckling loads of laminated circular cylindrical shells under mechanical and thermal loads, Donnell and improved Donnell equations were employed. Mohammad-Abadi and Daneshmehr [14] examined the free vibration and buckling of Bernoulli–Euler, Timoshenko, and Reddy beams based on the modified couple stress theory for several boundary conditions. They analytically solved governing equations compared the results with those of the generalized differential quadrature (GDQ) method. Using the zigzag theory and an improved third order theory (ITOT) by Dumir et al.[15], the thermal analysis of composite shells was investigated. Kant and Khare [16] and Khdeir et al. [17] described the thermoelastic behavior using classical or first-order theories. Khare et al. [18] thermo-mechanical analysis of simply supported doubly curved cross-ply laminated shells using of Closed-form formulations of 2D higher-order shear deformation theories are presented. The formulation includes the Sanders theory for doubly curved shells. Sheng and Wang [19] investigated the effect of thermal loading on the buckling and vibration of functionally graded cylindrical shells with a ring-stiffener, considering rotary inertia and transverse shear strains along the shell thickness. They also [20] thermoelastic vibration and buckling characteristics of the functionally graded piezoelectric cylindrical are investigated.

Recently, sandwich construction has become even more attractive due to the introduction of advanced composite materials for face sheets. As an example of the design of sandwich skins for aircraft wings, the prevention of buckling is very important. High-speed aircraft structural panels are subjected to not only aerodynamic loading, but also aerodynamic heating. Temperature rise may buckle the plate and reduce the load-carrying capacity. Shiau and Kuo In [21], the analysis of postbuckling behaviors of sandwich plates with composite laminated faces and honeycomb core subjected to a change in temperature was done. The thermal postbuckling behavior of a composite sandwich panel may be different from that of a composite laminated plate due to the introduction of laminated face and honeycomb core. The buckling responses of composite sandwich plates also analyzed by some researchers Shian [22], Rao [23]. Noor et al. [24] studied the nonlinear response of curved sandwich panels with composite face sheets subjected to a temperature gradient through the thickness combined with mechanical loadings. The analysis was based on a first-order shear-deformation Sanders-Budiansky-type theory, including the effects of large displacements, moderate rotations, transverse shear deformation, and laminated anisotropic material behavior. Chang [25] examined the thermal elastic behavior of a rectangular sandwich panel which was subjected to edge compression, transverse load, and high temperature difference between the two faces. Huang [26] and Huang and Kardomateas [27] used the ESL approach to analyze a sandwich panel allowing very large deformations. Frostig and Thomsen [28] examined the non-linear response of unidirectional sandwich panels with a ''soft'' core subjected to thermally induced deformation type of loading which might be fully distributed or localized. Khalili and Mohammadi [29] investigated the free vibration of sandwich plates with functionally graded (FG) face sheets in various thermal environments and employed improved high-order sandwich plate theory. Recently, the vibrations of a cylindrical sandwich shell with elastic core under local loads were studied by Ref [30].

Malekzadeh et al [31] presented the free vibrations and buckling behavior of the sandwich panel with a flexible core was investigated using a new improved high-order sandwich panel theory. In another work, jabbari et

al [32] thermo-elastic analysis of a rotating thick truncated conical shell subjected to the temperature gradient, internal pressure and external pressure. Based on rayleigh-ritz method, free vibration of partially fluid-filled laminated composite circular cylindrical shell with arbitrary boundary conditions investigated by [33]. Calculation of natural frequencies of bi-layered rotating functionally graded cylindrical shells is presented by Golpayegani [34]. The behavior of a graded cylindrical shell subjected to an axisymmetric thermo-electro-mechanical loading studied by [35]. They in this article, using the Fourier series expansion method, solved the governing and boundary conditions. Recently, buckling and post buckling of cylindrical shells under hydrostatic pressure investigated by Ghasemi et al [36]. They in this work, show that the shell with variable thickness has buckling pressure close to shell bucking pressure with mean thickness. Because of applications of sandwich panel structures under static and dynamic loads as well as for practical use in electrical engineering, materials science and construction engineering, this issue is considered.

To the best of our knowledge, no studies have been reported in the literature concerning the influence of boundary conditions on the vibration and buckling behavior of cylindrical sandwich panels under thermo-mechanical loadings. The purpose of the present study is investigating the effect of thermal loading on the buckling and vibration of a cylindrical sandwich panel with various boundary conditions using the first-order shear deformation theory (FSDT). the governing equations were solved by the GDQ method. The results were validated with those published in the literature and with the analytical method. Finally, influence of length-to-radius ratio, circumferential wave numbers, thermal loadings, and boundary conditions on the dynamic and static behavior of the cylindrical sandwich panel are examined.

## 2 FORMULATION

Fig. 1 shows a cylindrical sandwich panel. The thickness, length and the middle surface radius of the cylindrical sandwich panel are denoted by *h*, *L* and *R* respectively.

According to the FSDT, displacement fields of the cylindrical sandwich panel along $x$, $\theta$, and $z$ directions are expressed as [37]:

$$\begin{aligned} U(x,\theta,z,t) &= u(x,\theta,t) + z\,\psi_x(x,\theta,t) \\ V(x,\theta,z,t) &= v(x,\theta,t) + z\,\psi_\theta(x,\theta,t) \\ W(x,\theta,z,t) &= w(x,\theta,t) \end{aligned} \tag{1}$$

In which $u(x,\theta,t)$, $v(x,\theta,t)$ and $w(x,\theta,t)$ are the neutral surface displacements and $\psi_x(x,\theta,t)$ and $\psi_\theta(x,\theta,t)$ are the rotations about the axial and the circumferential directions, respectively. In addition, strain tensor is expressed as:

$$\varepsilon_{ij} = \frac{1}{2}(u_{i,j} + u_{j,i}) \tag{2}$$

Moreover, the stress–strain relation can be expressed as follows [38]:

$$\begin{bmatrix} \sigma_{xx} \\ \sigma_{\theta\theta} \\ \sigma_{x\theta} \end{bmatrix} = \begin{bmatrix} \bar{Q}_{11} & \bar{Q}_{12} & 0 \\ \bar{Q}_{12} & \bar{Q}_{22} & 0 \\ 0 & 0 & \bar{Q}_{44} \end{bmatrix}^{(L)} \begin{bmatrix} \varepsilon_{xx} \\ \varepsilon_{\theta\theta} \\ \varepsilon_{x\theta} \end{bmatrix}, \qquad \begin{bmatrix} \sigma_{\theta z} \\ \sigma_{xz} \end{bmatrix} = \begin{bmatrix} \bar{Q}_{66} & 0 \\ 0 & \bar{Q}_{55} \end{bmatrix}^{(L)} \begin{bmatrix} \varepsilon_{\theta z} \\ \varepsilon_{xz} \end{bmatrix} \tag{3}$$

In which the coefficients of the $\bar{Q}_{ij}$ matrix, known as the reduced elastic constants of the orthotropic material corresponding to *Lth* lamina, are expressed as follows:

$$
\begin{aligned}
\bar{Q}_{11} &= Q_{11}\cos^4\theta + 2(Q_{12}+2Q_{44})\sin^2\theta\cos^2\theta + Q_{22}\sin^4\theta \\
\bar{Q}_{12} &= (Q_{11}+Q_{22}-4Q_{44})\sin^2\theta\cos^2\theta + Q_{12}(\sin^4\theta+\cos^4\theta) \\
\bar{Q}_{22} &= Q_{11}\sin^4\theta + 2(Q_{12}+2Q_{44})\sin^2\theta\cos^2\theta + Q_{22}\cos^4\theta \\
\bar{Q}_{44} &= (Q_{11}+Q_{22}-2Q_{12})\sin^2\theta\cos^2\theta + Q_{44}(\cos^2\theta-\sin^2\theta)^2 \\
\bar{Q}_{55} &= Q_{55}\cos^4\theta + Q_{66}\sin^4\theta \\
\bar{Q}_{66} &= Q_{66}\cos^4\theta + Q_{55}\sin^4\theta
\end{aligned}
\tag{4}
$$

As mentioned earlier, the relations given by Eq. (3) are stress–strain constitutive relations for the *Lth* orthotropic lamina referred to as the lamina's principal material axes *x*, $\theta$, and *z*. In Eq (4), $\theta$ is fiber angel and $Q_{ij}$ is defined as follows:

$$
Q_{11} = \frac{E_1}{1-\nu_{12}\nu_{21}}, \quad Q_{12} = \frac{\nu_{12}E_2}{1-\nu_{12}\nu_{21}}, \quad Q_{22} = \frac{E_2}{1-\nu_{12}\nu_{21}}, \quad Q_{44} = G_{12}, \quad Q_{66} = G_{23}, \quad Q_{55} = G_{13} \tag{5}
$$

The stress-strain relation for the core is expressed as:

$$
\begin{Bmatrix} \sigma_{xx} \\ \sigma_{\theta\theta} \\ \sigma_{x\theta} \\ \sigma_{xz} \\ \sigma_{\theta z} \end{Bmatrix}^{core} = \begin{Bmatrix} E_{11}^c & 0 & 0 & 0 & 0 \\ 0 & E_{22}^c & 0 & 0 & 0 \\ 0 & 0 & G_{12}^c & 0 & 0 \\ 0 & 0 & 0 & G_{13}^c & 0 \\ 0 & 0 & 0 & 0 & G_{23}^c \end{Bmatrix}^{core} \begin{Bmatrix} \varepsilon_{xx} \\ \varepsilon_{\theta\theta} \\ 2\varepsilon_{x\theta} \\ 2\varepsilon_{xz} \\ 2\varepsilon_{\theta z} \end{Bmatrix}^{core} \tag{6}
$$

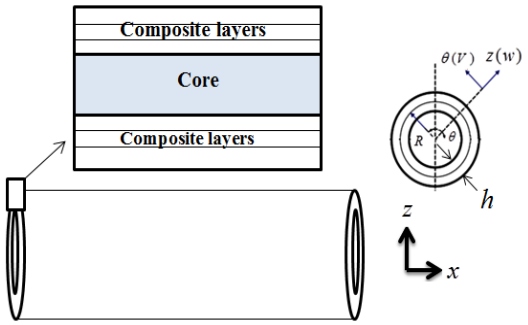


**Fig.1**
Geometry of the cylindrical sandwich panel.

The total stress for the cylindrical sandwich panel structure can be obtained from:

$$
\sigma_{ij}^{total} = \sigma_{ij}^{outer\ composit\ layers} + \sigma_{ij}^{Inner\ composit\ layers} + \sigma_{ij}^{core} \tag{7}
$$

It is worth mentioning that indices *i* and *j* in Eq. 7 are *x*, $\theta$, and *z* directions, respectively.

### *2.1 Governing equations and boundary conditions*

To derive the equations of motion and boundary conditions for the cylindrical sandwich panel using the first-order shear deformation shell model, one must insert the components of the displacement field into the strains. By substituting Eq. (1) into Eq. (2), the components of strain tensor are obtained as follows:

$$\begin{aligned}
\varepsilon_{xx} &= \frac{\partial u}{\partial x} + z\,\frac{\partial \psi_x}{\partial x} \\
\varepsilon_{\theta\theta} &= \frac{1}{R}\frac{\partial v}{\partial \theta} + z\,\frac{1}{R}\frac{\partial \psi_\theta}{\partial \theta} + \frac{w}{R} \\
\varepsilon_{xz} &= \frac{1}{2}(\psi_x + \frac{\partial w}{\partial x}) \\
\varepsilon_{x\theta} &= \frac{1}{2}(\frac{1}{R}\frac{\partial u}{\partial \theta} + \frac{\partial v}{\partial x}) + \frac{z}{2}(\frac{1}{R}\frac{\partial \psi_x}{\partial \theta} + \frac{\partial \psi_\theta}{\partial x}) \\
\varepsilon_{\theta z} &= \frac{1}{2}(\psi_\theta + \frac{1}{R}\frac{\partial w}{\partial \theta} - \frac{v}{R})
\end{aligned} \tag{8}$$

In Eq. (8), the mean of $R$ is the average of the radius of the cylindrical sandwich panel. For the equations of motion and boundary conditions, the principle of minimum potential energy states that [39]:

$$\int_{t_1}^{t_2}(\delta T - \delta U + \delta W_1 + \delta W_2)dt = 0 \tag{9}$$

where $\delta T$ , $\delta U$ , $\delta W_1$ and $\delta W_2$ are the variations of kinetic energy, strain energy, and the work of external forces due to mechanical and temperature loading, respectively. The strain energy of the cylindrical sandwich panel is expressed as follows:

$$\delta U = \frac{1}{2}\iiint_V(\sigma_{ij}\,\delta\varepsilon_{ij})dV = \iint_A \left\{ \begin{array}{l} (N_{xx}\,\dfrac{\partial}{\partial x}\delta u + M_{xx}\,\dfrac{\partial}{\partial x}\delta\psi_x) + N_{\theta\theta}(\dfrac{1}{R}\dfrac{\partial}{\partial\theta}\delta v + \dfrac{\delta w}{R}) + \\ M_{\theta\theta}\,\dfrac{1}{R}\dfrac{\partial}{\partial\theta}\delta\psi_\theta + Q_{xz}(\delta\psi_x + \dfrac{\partial}{\partial x}\delta w) + \\ N_{x\theta}(\dfrac{1}{R}\dfrac{\partial}{\partial\theta}\delta u + \dfrac{\partial}{\partial x}\delta v) + M_{x\theta}(\dfrac{1}{R}\dfrac{\partial}{\partial\theta}\delta\psi_x + \dfrac{\partial}{\partial x}\delta\psi_\theta) \\ +Q_{z\theta}(\delta\psi_\theta + \dfrac{1}{R}\dfrac{\partial}{\partial\theta}\delta w - \dfrac{\delta v}{R}) \end{array} \right\} R\,dx\,d\theta \tag{10}$$

where force and momentum are defined as follows:

$$\begin{aligned}
(N_{xx}, N_{\theta\theta}, N_{x\theta}) &= \int_{-h/2}^{h/2}(\sigma_{xx}, \sigma_{\theta\theta}, \sigma_{x\theta})dz\,, \\
(M_{xx}, M_{\theta\theta}, M_{x\theta}) &= \int_{-h/2}^{h/2}(\sigma_{xx}, \sigma_{\theta\theta}, \sigma_{x\theta})z\,dz\,, \\
(Q_{xz}, Q_{z\theta}) &= \int_{-h/2}^{h/2}k_s(\sigma_{xz}, \sigma_{z\theta})dz\,,
\end{aligned} \tag{11}$$

In the above equation, $k_s$ is the shear correction factor. In addition, to obtain admissible results, the shear correction factor is considered to be $k_s$ =5/6 [40]. Also, the kinetic energy of a cylindrical sandwich panel can be expressed as:

$$\delta T = \int_Z \iint_A \rho \left\{ \begin{array}{l} (\dfrac{\partial u}{\partial t} + z\,\dfrac{\partial \psi_x}{\partial t})(\dfrac{\partial}{\partial t}\delta u + z\,\dfrac{\partial}{\partial t}\delta\psi_x) \\ +(\dfrac{\partial v}{\partial t} + z\,\dfrac{\partial \psi_\theta}{\partial t})(\dfrac{\partial}{\partial t}\delta v + z\,\dfrac{\partial}{\partial t}\delta\psi_\theta) + (\dfrac{\partial w}{\partial t})\dfrac{\partial}{\partial t}\delta w \end{array} \right\} R\,dz\,dx\,d\theta \tag{12}$$

Furthermore, the work done by the mechanical loading can be written as:

$$\delta W_1 = \int_0^L \int_0^{2\pi} F\left(\frac{\partial^2 v}{\partial x^2}\delta v + \frac{\partial^2 w}{\partial x^2}\delta w\right) R\,d\theta\,dx \tag{13}$$

In the above equation, $F$ is the mechanical loading which is constant. Temperature distribution in the cylindrical sandwich panel can be obtained by solving the following steady-state heat-transfer equation:

$$-\frac{d}{dz_i}\left(k_i \frac{dT_i}{dz_i}\right)=0;\ i=t,c,b \tag{14}$$

In this paper, $t$, $c$, and $b$ mean the outer composite layer, core, and inner composite layer of the cylindrical sandwich panel, respectively. Also, $K$ is the thermal conductivity coefficient of the structure. Boundary conditions for transfer heat are expressed as follows:

$$\begin{aligned}
&T_t\left(z_t=\frac{h_t}{2}\right)=T_u\\
&T_b\left(z_b=\frac{-h_b}{2}\right)=T_l\\
&T_b\left(z_b=\frac{h_b}{2}\right)=T_c\left(z_c=\frac{-h_c}{2}\right)\\
&T_t\left(z_t=\frac{-h_t}{2}\right)=T_c\left(z_c=\frac{h_c}{2}\right)\\
&k_t\frac{dT_t}{dz_t}\bigg|z_t=\frac{-h_t}{2}=k_c\frac{dT_c}{dz_c}\bigg|z_t=\frac{h_c}{2}\\
&k_b\frac{dT_b}{dz_b}\bigg|z_b=\frac{h_b}{2}=k_c\frac{dT_c}{dz_c}\bigg|z_t=\frac{-h_c}{2}\\
&h_t+h_c+h_b=h
\end{aligned} \tag{15}$$

In Eq. (15), $T_u$, $T_b$ and $T_c$ are the temperatures of outer, inner, and core of the cylindrical sandwich panel. Moreover, $k_u$, $k_b$ and $k_c$ are the thermal conductivity coefficients of the structure. By substituting Eq. (15) into Eq. (14), the temperature distribution function for outer and inner composite layers and core of the cylindrical sandwich panel are expressed as follows:

$$\begin{aligned}
&T_t(x,\theta,z)=T_t^0(x,\theta)+T_t^I(x,\theta)z_t\\
&T_c(x,\theta,z)=T_c^0(x,\theta)+T_c^I(x,\theta)z_c\\
&T_t(x,\theta,z)=T_t^0(x,\theta)+T_t^I(x,\theta)z_t\\
&T_b(x,\theta,z)=T_b^0(x,\theta)+T_b^I(x,\theta)z_b
\end{aligned} \tag{16}$$

Now by substituting Eq. (15) into Eq. (16), the temperature changes ($T_u-T_l$), between outer and inner surfaces of the cylindrical sandwich panel can be obtained. Hence, the first variation of the work done corresponding to temperature change can be expressed as [20, 41]:

$$\delta W_2=\iint_A\left[N_1^{Total}\frac{\partial w}{\partial x}\frac{\partial \delta w}{\partial x}+N_2^{Total}\frac{\partial v}{\partial x}\frac{\partial \delta v}{\partial x}\right]R\,dx\,d\theta a \tag{17}$$

where $N_1^T$ and $N_2^T$ are thermal resultants. Note that the two thermal resultants are equal and can be expressed as:

$$
\begin{aligned}
&N_i^T = \int_{-h_i/2}^{h_i/2} \left(\bar{Q}_{11} + \bar{Q}_{12}\right)(\alpha_{xx})(T_i - T_{ref})dz\,,\ i = t,b\\
&N_i^{2T} = \int_{-h_i/2}^{h_i/2} \left(\bar{Q}_{21} + \bar{Q}_{22}\right)(\alpha_{\theta\theta})(T_i - T_{ref})dz\,,\ i = t,b\\
&N_c^T = \int_{-h_c/2}^{h_c/2} \left(E_{11}^c\right)(\alpha_{xx}^c)(T_c - T_{ref})dz\,,\\
&N_c^{2T} = \int_{-h_c/2}^{h_c/2} \left(E_{22}^c\right)(\alpha_{\theta\theta}^c)(T_c - T_{ref})dz\,,\\
&N_1^{Total} = N_i^T + N_c^T\\
&N_2^{Total} = N_i^{2T} + N_c^{2T}
\end{aligned}
\tag{18}
$$

Thermal expansion coefficients are given by:

$$
\begin{aligned}
&\alpha_{xx} = \alpha_1 \cos^2\theta + \alpha_2 \sin^2\theta\\
&\alpha_{\theta\theta} = \alpha_1 \sin^2\theta + \alpha_2 \cos^2\theta
\end{aligned}
\tag{19}
$$

By substituting Eqs. (10), (12), (13), (17) into Eq. (9) and integrating by parts, the equations of motion and boundary conditions can be obtained as follows, using the first-order shear deformation sandwich panel model:

$$
\begin{aligned}
&\delta u: \frac{\partial N_{xx}}{\partial x} + \frac{1}{R}\frac{\partial N_{x\theta}}{\partial \theta} = I_0 \frac{\partial^2 u}{\partial t^2} + I_1 \frac{\partial^2 \psi_x}{\partial t^2}\\
&\delta v: \frac{\partial N_{x\theta}}{\partial x} + \frac{1}{R}\frac{\partial}{\partial \theta}N_{\theta\theta} + \frac{Q_{z\theta}}{R} - \left(N_2^{total} + F\right)\frac{\partial^2 v}{\partial x^2} = I_0 \frac{\partial^2 v}{\partial t^2} + I_1 \frac{\partial^2 \psi_\theta}{\partial t^2}\\
&\delta w: \frac{\partial Q_{xz}}{\partial x} + \frac{1}{R}\frac{\partial Q_{z\theta}}{\partial \theta} - \frac{N_{\theta\theta}}{R} - \left(N_1^{total} + F\right)\frac{\partial^2 w}{\partial x^2} = I_0 \frac{\partial^2 w}{\partial t^2}\\
&\delta \psi_x: \frac{\partial M_{xx}}{\partial x} + \frac{1}{R}\frac{\partial M_{x\theta}}{\partial \theta} - Q_{xz} = I_1 \frac{\partial^2 u}{\partial t^2} + I_2 \frac{\partial^2 \psi_x}{\partial t^2}\\
&\delta \psi_\theta: \frac{1}{R}\frac{\partial M_{\theta\theta}}{\partial \theta} + \frac{\partial M_{x\theta}}{\partial x} - Q_{z\theta} = I_1 \frac{\partial^2 v}{\partial t^2} + I_2 \frac{\partial^2 \psi_\theta}{\partial t^2}
\end{aligned}
\tag{20}
$$

Boundary conditions are listed below:

$$
\begin{aligned}
&\delta u = 0 \quad or \quad (N_{xx})n_x + (N_{x\theta})n_\theta = 0,\\
&\delta v = 0 \quad or \quad (N_{x\theta})n_x + (N_{\theta\theta})n_\theta = 0,\\
&\delta w = 0 \quad or \quad (Q_{xz})n_x + (Q_{\theta z})n_\theta = 0,\\
&\delta \psi_x = 0 \quad or \quad (M_{xx})n_x + (M_{\theta x})n_\theta = 0,\\
&\delta \psi_\theta = 0 \quad or \quad (M_{x\theta})n_x + (M_{\theta\theta})n_\theta = 0
\end{aligned}
\tag{21}
$$

## 3 SOLUTION PROCEDURE

In this section, the summarized explanation of numerical and analytical solutions of governing equations is stated. The numerical solution is obtained using the GDQ method and analytical solution based on Navier method for a cylindrical circular composite sandwich panel simply supported on all the edges.

### *3.1 Numerical solution procedure*

Differential quadrature method (DQM) is an accurate and effective numerical method presented in early 1970s [42, 43]. The accuracy of this method depends on its weighting coefficients precision controlled by the number of grid

points. In primary formulations of DQM, an algebraic equation system was employed to calculate weighting coefficients which determined the number of grid points. An explicit formulation for the weighting coefficients was later presented by Shu [44], and led to GDQ. Many regular domain problems are solved using this procedure. Shu and Richards [45] developed a domain parsing method to be applied in multi-domain problems. Therefore, a number of sub-domains are obtained by main domain division before discretizing each sub-domain for GDQ. The *r-th* order derivatives of a function $f(x_i)$ is achieved as below [44]:

$$\left.\frac{\partial^r f(x)}{\partial x^r}\right|_{x=x_P} = \sum_{j=1}^{s} C_{ij}^{(r)} f(x_i) \tag{22}$$

where *s* is the number of grid points along the *x* direction. In addition, $C_{ij}$ is obtained as follows:

$$C_{ij}^{(1)} = \begin{cases} \dfrac{M(r_i)}{(r_i - r_j) M(r_j)} & i \neq j \\ -\sum\limits_{j=1, i\neq j}^{s} C_{ij}^{(1)} & i = j \end{cases} \tag{23}$$

and *M* is defined as:

$$M(x_i) = \prod_{j=1, j\neq i}^{s} (x_i - x_j) \tag{24}$$

Superscript *"r"* is the order of the derivative. Furthermore, $C^{(r)}$ is the weighing coefficient along the *x* direction, which can be written as:

$$C_{ij}^{(r)} = \begin{cases} r\left[C_{ij}^{(r-1)} C_{ij}^{(1)} - \dfrac{C_{ij}^{(r-1)}}{(r_i - r_j)}\right] & i \neq j \text{ and } 2 \leq r \leq s-1 \\ -\sum\limits_{j=1, i\neq j}^{s} C_{ij}^{(r)} & i = j \text{ and } 1 \leq r \leq s-1 \end{cases} \tag{25}$$

A better mesh point distribution is acquired based on Chebyshev-Gauss-Lobatto technique:

$$x_i = \frac{L}{2}\left(1 - \cos\left(\frac{(i-1)}{(S_i - 1)}\pi\right)\right) \qquad i = 1, 2, 3, \ldots, S_i \tag{26}$$

The degrees of freedom can be assumed as follows:

$$\begin{aligned} u(x,\theta,t) &= \sum_{i}^{S} U(x_i) \sin(n\theta) e^{i\omega t}, \\ v(x,\theta,t) &= \sum_{i}^{S} V(x_i) \cos(n\theta) e^{i\omega t}, \\ w(x,\theta,t) &= \sum_{i}^{S} W(x_i) \sin(n\theta) e^{i\omega t}, \\ \psi_x(x,\theta,t) &= \sum_{i}^{S} \Psi_x(x_i) \cos(n\theta) e^{i\omega t}, \\ \psi_\theta(x,\theta,t) &= \sum_{i}^{S} \Psi_\theta(x_i) \sin(n\theta) e^{i\omega t}. \end{aligned} \tag{27}$$

The governing equations of the cylindrical sandwich panel based on GDQ method into, i.e. Eq. (20) are applied. The natural frequency and buckling of the structure were calculated with the solution of the proposed eigenvalue equation in the form of Eq. (28).

$$\begin{aligned} &\left[K_g\right]N_{cr}+\left[K\right]=0 \\ &\left[M\right]\omega^2+\left[K\right]=0 \end{aligned} \tag{28}$$

*3.2 Analytical solution*

In order to obtain the natural frequencies and critical loading of the simply supported cylindrical sandwich panel, the Navier method was applied. In order to satisfy the boundary conditions, the displacement fields based on double Fourier series were assumed to be in the following form:

$$\begin{Bmatrix} u(x,\theta,t) \\ v(x,\theta,t) \\ w(x,\theta,t) \\ \psi_x(x,\theta,t) \\ \psi_\theta(x,\theta,t) \end{Bmatrix} = \sum_{m=1}^{\infty}\sum_{n=1}^{\infty} \begin{Bmatrix} U_{mn}\cos(\frac{m\pi}{L}x)\cos(n\theta) \\ V_{mn}\sin(\frac{m\pi}{L}x)\sin(n\theta) \\ W_{mn}\sin(\frac{m\pi}{L}x)\cos(n\theta) \\ \Psi_{x\,mn}\cos(\frac{m\pi}{L}x)\cos(n\theta) \\ \Psi_{\theta mn}\sin(\frac{m\pi}{L}x)\sin(n\theta) \end{Bmatrix} \tag{29}$$

where *m* is the axial half-wave number and n is the circumferential wave number. Substituting Eq. (29) into Eq. (20), a characteristic equation for buckling loads and natural frequencies can be obtained. The minimum eigenvalue of Eq. (28) is the buckling load and fundamental natural frequency of sandwich cylindrical panel which is determined using MATLAB code.

The Material properties of a cylindrical sandwich panel with an elastic core are given in Table 1.

**Table1**
Material properties of a cylindrical sandwich panel.

| | |
|---|---|
| Material properties of core: | $E_1 = E_2 = E_3 = 0.00689\ Gpa,\ G_{12} = G_{13} = G_{23} = 0.00345\ GPa$<br>$\nu = 10^{-5}$ , $\rho = 94.195\ Kg/m^3$ |
| Material properties of composite layers: | $E_1 = 131\ GPa, E_2 = E_3 = 10.34\ GPa,\ G_{12} = G_{13} = 6.895\ GPa, G_{23} = 6.205 GPa,$<br>$\nu_{12} = \nu_{13} = 0.22$ , $\nu_{23} = 0.49$ , $\rho = 1627\ kg/m^3$ |

## 4 RESULTS AND DISCUSSION

In this section, the numerical results of the vibration behavior of the cylindrical sandwich panel are investigated for various boundary conditions. A sufficient number of grid points is necessary to achieve accurate results in the GDQ method. For the free vibration analysis of the cylindrical sandwich panel, as it is shown in Table 2., for the good results, 35 grid points are appropriate. In addition, 30 grid points are necessary for buckling load analysis of the cylindrical sandwich panel, as presented in Table 3. The Results are presented and analyzed in two sections. The first section verifies the proposed model with the presented analytical model and existing literature. The second section shows the effect of some factors on critical buckling load and natural frequency of the cylindrical sandwich panel. The said factors are the length-to-radius ratio, radius-to-thickness ratio, thermal and mechanical loadings, circumferential mode number, and boundary conditions.

**Table2**
The effect of the number of grid points on evaluating the convergence of natural frequency (*Hz*) of the cylindrical sandwich panel with respect to different mechanical and thermal loadings, boundary conditions (B.Cs), and $L / R$ =10, $h / R$ =0.1, $h_e / h$ =0.5, $h_t = h_b$ and $n$=1.

| Boundary condition | Mechanical loading | Thermal loading | $S$=20 | $S$=25 | $S$=30 | $S$=35 | $S$=40 | $S$=45 | $S$=50 |
|---|---|---|---|---|---|---|---|---|---|
| Simply-Simply | $F$=$1\times10^6$ | $\Delta T$ =100 | 549.704 | 549.704 | 549.704 | 549.704 | 549.704 | 549.704 | 549.704 |
| | $F$=$2\times10^6$ | $\Delta T$ =200 | 471.236 | 471.236 | 471.236 | 471.236 | 471.236 | 471.236 | 471.236 |
| Simply-Clamp | $F$=$1\times10^6$ | $\Delta T$ =100 | 722.984 | 722.957 | 722.963 | 722.962 | 722.962 | 722.962 | 722.962 |
| | $F$=$2\times10^6$ | $\Delta T$ =200 | 662.524 | 662.493 | 662.500 | 662.498 | 662.498 | 662.498 | 662.498 |
| Clamp-Clamp | $F$=$1\times10^6$ | $\Delta T$ =100 | 890.331 | 890.332 | 890.333 | 890.333 | 890.333 | 890.333 | 890.333 |
| | $F$=$2\times10^6$ | $\Delta T$ =200 | 841.458 | 841.459 | 841.460 | 841.460 | 841.460 | 841.460 | 841.460 |

**Table3**
The effect of the number of grid points on evaluating the convergence of dimensionless buckling loading of the cylindrical sandwich panel with respect to different length-to-radius ratios, circumferential mode numbers, boundary conditions (B.Cs), and $h / R$ =0.1, $h_e / h$ =0.5, $h_t = h_b$ , $L / R$ =10 and $\bar{N}_{cr} = 100 \cdot N_{cr} R^3 / E_{1t} h^3$ .

| B.C | circumferential Mode number ($n$) | $S$=20 | $S$=25 | $S$=30 | $S$=35 | $S$=40 | $S$=45 | $S$=50 |
|---|---|---|---|---|---|---|---|---|
| Simply-Simply | 1 | 4.8755 | 4.8755 | 4.8755 | 4.8755 | 4.8755 | 4.8755 | 4.8755 |
| | 3 | 12.1853 | 12.1808 | 12.1808 | 12.1853 | 12.1808 | 12.1808 | 12.1853 |
| Simply-Clamp | 1 | 7.2390 | 7.2387 | 7.2388 | 7.2388 | 7.2388 | 7.2388 | 7.2388 |
| | 3 | 12.1870 | 12.1846 | 12.1846 | 12.1846 | 12.1846 | 12.1846 | 12.1846 |
| Clamp-Clamp | 1 | 10.1817 | 10.1817 | 10.1817 | 10.1817 | 10.1817 | 10.1817 | 10.1817 |
| | 3 | 12.2455 | 12.2431 | 12.2431 | 12.2431 | 12.2431 | 12.2431 | 12.2431 |

*4.1 Verification of results using the results of an analytical method*

In this section, GDQ results are validated with the results of the present analytical solution. Tables 4 and 5 demonstrate GDQ results in comparison with analytical results for different parameters of the cylindrical sandwich panel. It can be seen from Tables 4 and 5 that the GDQ results are in accordance with analytical results. Therefore, the GDQ method with $N$=35 can be used instead of an analytical solution. Moreover, it can be seen clearly from Table 4 that, by increasing temperature change, the natural frequency tends to decrease and increases when mechanical loading decreases. The comparison of natural frequencies presented in Table 4 reveals that an increase in the length-to-radius ratio of the cylindrical sandwich panel leads to a decrease in stiffness and, therefore, a decrease in natural frequency. Furthermore, in the present study, dimensionless frequency is approximated by Eq. $\Omega = \omega L^2 \sqrt{\rho_t / E_{2t}}$ .

**Table4**
The comparison of non-dimensional first natural frequencies obtained by analytical and GDQ methods for the cylindrical sandwich panel with $h / R$ =0.1, $h_e / h$ =0.5, $h_t = h_b$ and $n$=1.

| $\Delta T$ | | 100 | | 200 | | 300 | | 400 | |
|---|---|---|---|---|---|---|---|---|---|
| $L / R$ | $F(N)$ | Analytical | GDQ | Analytical | GDQ | Analytical | GDQ | Analytical | GDQ |
| 10 | 1e6 | 0.218053 | 0.218142 | 0.210615 | 0.210706 | 0.202903 | 0.202997 | 0.194886 | 0.194984 |
| | 1.2e6 | 0.213691 | 0.213781 | 0.206095 | 0.206188 | 0.198208 | 0.198304 | 0.189993 | 0.190092 |
| | 1.4e6 | 0.209239 | 0.209330 | 0.201474 | 0.201569 | 0.193398 | 0.193496 | 0.184970 | 0.185072 |
| | 1.6e6 | 0.204689 | 0.204782 | 0.196745 | 0.196842 | 0.188466 | 0.188567 | 0.179806 | 0.179911 |
| 12 | 1e6 | 0.175627 | 0.175716 | 0.164256 | 0.16435 | 0.152036 | 0.152137 | 0.138744 | 0.138854 |
| | 1.2e6 | 0.169044 | 0.169136 | 0.157197 | 0.157295 | 0.144381 | 0.144487 | 0.130310 | 0.130426 |
| | 1.4e6 | 0.162194 | 0.162289 | 0.149806 | 0.149908 | 0.136296 | 0.136408 | 0.121290 | 0.121415 |
| | 1.6e6 | 0.155041 | 0.15514 | 0.14203 | 0.142138 | 0.127700 | 0.127819 | 0.111544 | 0.111679 |
| 14 | 1e6 | 0.134813 | 0.134906 | 0.116746 | 0.116853 | 0.095314 | 0.0954434 | 0.067377 | 0.0675588 |
| | 1.2e6 | 0.124570 | 0.12467 | 0.104751 | 0.104869 | 0.080173 | 0.080326 | 0.043381 | 0.0436686 |
| | 1.4e6 | 0.113405 | 0.113514 | 0.0911903 | 0.0913253 | 0.061405 | 0.0616039 | 0.000000 | 0.000000 |
| | 1.6e6 | 0.101013 | 0.101135 | 0.0752237 | 0.0753864 | 0.033361 | 0.0337311 | 0.000000 | 0.000000 |

In order to verify the results of the critical buckling load of the cylindrical sandwich panel, the model represented in this study can be validated with the results obtained from the exact solution. Note that the dimensionless critical buckling load is defined according to $\bar{N}_{cr} = 100 \cdot N_{cr} R^3 / E_{1t} h^3$. It is worth mentioning that, using the GDQ solution, results have the maximum error of 1.9% compared to the exact solution results. Critical buckling loads provided by the present model are very close to the values of the exact solution. Moreover, it can be observed from Table 5 that, by increasing the core thickness-to-total thickness ratio, dimensionless buckling load tends to decrease, because the stiffness of the structure and the critical buckling load decrease by increasing this ratio. In addition, by increasing the number of layers of the cylindrical sandwich panel structure, the critical buckling load increases.

**Table5**
The comparison of dimensionless buckling loading of simply supported cylindrical sandwich panel for different thickness ratios of core and composite layer when $h / R$ =0.1, $h_t = (h - h_c)/2$, $h_b = h_t$, $L / R$ =10, $\Delta T$ =0 and $n$=1.

| $h_c / h$ | Exact solution ($N_1$ =2) | GDQ solution ($N_1$ =2) | Error % | Exact solution ($N_1$ =3) | GDQ solution ($N_1$ =3) | Error % |
|---|---|---|---|---|---|---|
| 0.2 | 7.114349 | 0.0063 | 0.0449 | 7.935709 | 7.785030 | 0.0190 |
| 0.3 | 6.249844 | 0.0063 | 0.0392 | 6.947589 | 6.815744 | 0.0190 |
| 0.4 | 5.378515 | 0.0063 | 0.0336 | 5.958973 | 5.845963 | 0.0190 |
| 0.5 | 4.500314 | 0.0062 | 0.0280 | 4.969668 | 4.875493 | 0.0189 |
| 0.6 | 3.615199 | 0.0062 | 0.0224 | 3.979481 | 3.904141 | 0.0189 |
| 0.7 | 2.723139 | 0.0062 | 0.0168 | 2.98822 | 2.931715 | 0.0189 |
| 0.8 | 1.824106 | 0.0061 | 0.0112 | 1.995694 | 1.958024 | 0.0189 |
| 0.9 | 0.9180801 | 0.0061 | 0.0056 | 1.001711 | 0.9828757 | 0.0188 |
| 1.0 | 0.0023838 | 0.0000 | 0.0000 | 0.0023838 | 0.0023838 | 0.0000 |

Also, for the verification of the results of this work with those obtained by [46], Table 6 gives a comparison of results for the nondimensional frequency of simply supported homogeneous cylindrical shell.

**Table6**
Comparison of nondimensional natural frequency of cylindrical shells for different values of circumferential wave number ($n$) with $L / R$ =20, $R / h$ =100.

| $n$ | Loy et al. [46] | Present | Error (%) |
|---|---|---|---|
| 1 | 0.016101 | 0.0158099 | 0.18 |
| 2 | 0.009382 | 0.0092548 | 1.36 |
| 3 | 0.022105 | 0.0217143 | 0.17 |
| 4 | 0.042095 | 0.0413625 | 0.17 |

For another verification, Table 7 show the obtained results for natural frequency of the simply supported cylindrical shell for a different range of FG power index ($F$), length to radius ratio and theories. As shown in this table, there are good agreement between presented study (FSDT) with calssic and high order shear deformation shell theories. When the comparison between classic, FSD and HSD theories, is taken into account, it can be deduced that while a theory changes from classic to FSDT and from FSDT to HSDT the natural frequencies decrease.

**Table 7**
Comparison of the fundamental natural frequencies ($Hz$) for different cylindrical shell theory against $h / R$ ratios with ($L / R$ =20).

| | $h / R$ | $F$=0 | $F$=0.5 | $F$=0.7 | $F$=1 | $F$=2 | $F$=5 | $F$=15 |
|---|---|---|---|---|---|---|---|---|
| Classical theory [47] | 0.020 | 13.552 | 13.325 | 13.273 | 13.215 | 13.107 | 13.001 | 12.936 |
| | 0.030 | 13.557 | 13.330 | 13.278 | 13.220 | 13.112 | 13.006 | 12.941 |
| | 0.040 | 13.563 | 13.336 | 13.284 | 13.226 | 13.119 | 13.013 | 12.948 |
| | 0.050 | 13.572 | 13.345 | 13.293 | 13.235 | 13.127 | 13.021 | 12.956 |
| Higher-order deformation theory [48] | 0.020 | 13.4172 | 13.1924 | 13.1405 | 13.0828 | 12.9758 | 12.8710 | 12.8065 |
| | 0.030 | 13.4220 | 13.1971 | 13.1451 | 13.0874 | 12.9804 | 12.8756 | 12.8111 |
| | 0.040 | 13.4287 | 13.2037 | 13.1517 | 13.0939 | 12.9869 | 12.8820 | 12.8175 |
| | 0.050 | 13.4373 | 13.2121 | 13.1601 | 13.1023 | 12.9952 | 12.8903 | 12.8257 |
| First order deformation theory (Present) | 0.020 | 13.5156 | 13.2894 | 13.2375 | 13.1797 | 13.0722 | 12.9668 | 12.9019 |
| | 0.030 | 13.5204 | 13.2941 | 13.2422 | 13.1845 | 13.0769 | 12.9715 | 12.9065 |
| | 0.040 | 13.5271 | 13.3008 | 13.2489 | 13.1911 | 13.0835 | 12.9780 | 12.9130 |
| | 0.050 | 13.5356 | 13.3093 | 13.2574 | 13.1995 | 13.0919 | 12.9863 | 12.9212 |

*4.2 Parametric results*

In this section, the effect of boundary conditions on natural frequency and critical buckling load for different parameters are presented. Fig. 2 demonstrates a presentation of the effect of temperature changes on dimensionless natural frequency under various boundary conditions. As it can be seen from Fig. 2, an increase in temperature changes leads to a decrease in the dimensionless frequency in the first mode. This trend is observed under all types of boundary conditions. This is because increasing temperature changes eventuates in a decrease in the stiffness and natural frequency of the cylindrical sandwich panel in the stability area. The Simply-Simply boundary condition has the lowest frequency because of its particular condition, and the Clamp-Clamp boundary condition has the highest frequency. A surprising result is that the Simply-Simply boundary condition causes a decrease in the stability, and the Clamp-Clamp boundary condition causes an increase in the stability of the cylindrical sandwich panel. In addition, because of the damping in the structure, imaginary part of frequency occurs. The imaginary part is corresponding to the system damping, and the real part representing the system frequencies. For more explanation, according to ref [49], as the eigenfrequencies have the positive imaginary parts, which the system becomes unstable. In this state, both real and imaginary parts of frequency become zero at the same point. Therefore, with increasing axial load, system stability decreases and became susceptible to buckling.

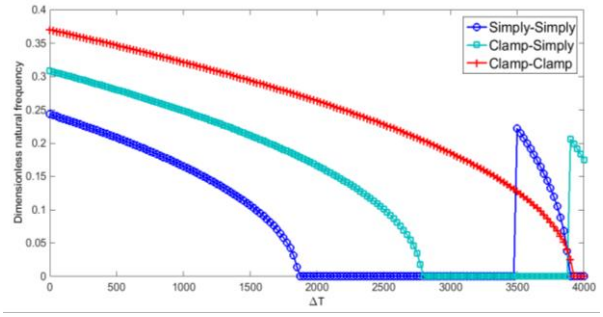


**Fig.2**
The variation of dimensionless fundamental frequency versus the temperature change of a cylindrical sandwich panel with different boundary conditions when $L$=1; $R$=0.1$L$; $h$=0.1$R$; $h_c = h / 2$ and $F$=1e5.

Figs. 3 and 4 illustrate the real and imaginary parts of natural frequency mechanical loading for different length-to-radius ratios. It is worth mentioning that the real part is related to natural frequency and the imaginary part is related to damping. It can be seen from the graph that, as the mechanical loading increases, the real part of natural frequency decreases, leading to an increase in the instability of the cylindrical sandwich panel. This is due to the increase in the rigidity of the cylindrical sandwich panel.

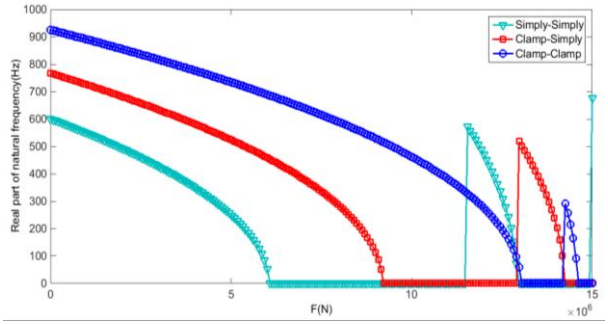


**Fig.3**
The variation of the real part of fundamental frequency versus the mechanical loading of a cylindrical sandwich panel with different boundary conditions when $L$=1; $R$=0.1$L$; $h$=0.1$R$; $h_c = h / 2$ and $\Delta T$ =100.

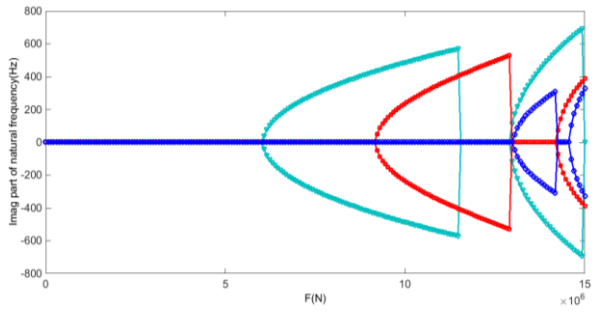


**Fig.4**
The variation of the imaginary part of fundamental frequency versus the mechanical loading of a cylindrical sandwich panel with different boundary conditions when $L$=1; $R$=0.1$L$; $h$=0.1$R$; $h_c = h / 2$ and $\Delta T$ =100.

Fig. 5 gives a presentation of circumferential wave numbers' effect and boundary condition on natural frequency under various laminated layers. According to Fig. 5, an increase in laminated layer leads to an increase in the frequency of all modes. This trend is observed under all types of boundary conditions because increasing the number of layers eventuates in an increase in the stiffness and natural frequency of the cylindrical sandwich panel. In addition, the increase in the modes of frequency results in a considerable increase in natural frequency. A surprising result is that, by increasing the circumferential mode number, the natural frequency first decreases and then increases as the circumferential wave number tends to increase. It is noted that the fundamental natural frequency occurs at $n$=2. The Simply-Simply boundary condition and the Clamp-Clamp boundary condition have the lowest and highest frequencies, respectively.

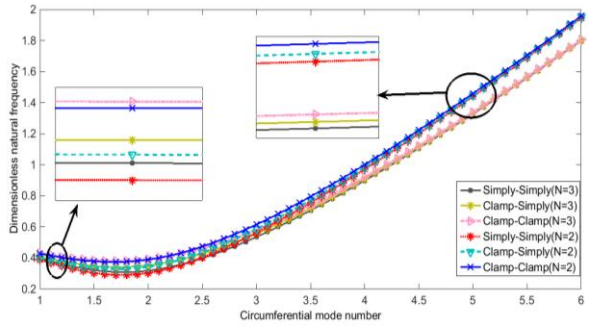


**Fig.5**
The variation of dimensionless fundamental frequency versus the mode number of a cylindrical sandwich panel with different composite layers and boundary conditions when $L$=1; $R$=$L$/3; $h$=0.1$R$; $h_c = h/2$; $T$=100; $F$=1e5.

Another parametric study is related to the study of variation of dimensionless critical buckling load versus the length-to-radius ratio, variation of temperature, and circumferential wave number ($n$), depicted in Figs. 5, 6, and 7, respectively. Based on Fig. 6, due to the enhancement in the length and decrease in the stiffness of the panel, the variation of dimensionless critical buckling load versus the length-to-radius ratio of a cylindrical sandwich panel with different boundary conditions decreases.

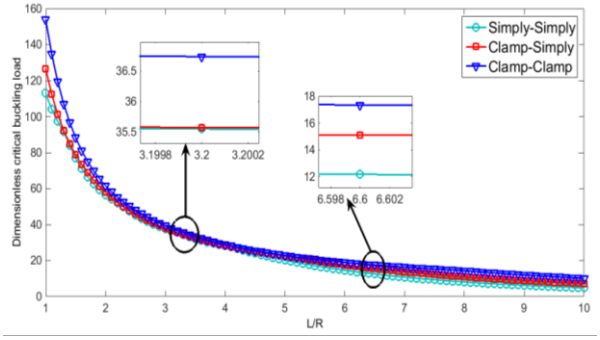


**Fig.6**
The variation of dimensionless critical buckling load versus the length-to-radius ratio of a cylindrical sandwich panel with different boundary conditions when $L$=1; $h$=0.1$R$; $h_c = h/2$ and $T$=100.

Studies have been carried out on the cylindrical sandwich panel to understand the behavior of dimensionless critical buckling load variation with respect to temperature in various boundary conditions. It is clear from Fig. 7 that, because of the decrease in the stiffness panel with rising the temperature, the variation of dimensionless critical buckling load decreases with the increase in temperature.

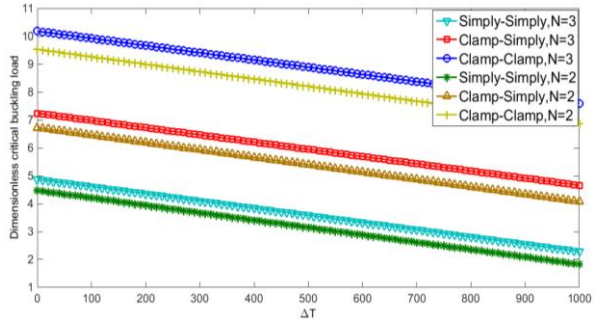


**Fig.7**
The variation of dimensionless critical buckling load versus the temperature change of a cylindrical sandwich panel with different composite layers and boundary conditions when $L$=1; $R$=0.1$L$; $h$=0.1$R$; $h_c = h/2$; $n$=1.

Variation of the dimensionless critical buckling load versus circumferential wave number ($n$) for different boundary conditions is depicted in Fig. 8. It can be seen that, by increasing the circumferential wave number, the dimensionless critical buckling load of the sandwich panel initially decreases and then increases when $n$ reaches a specific magnitude.

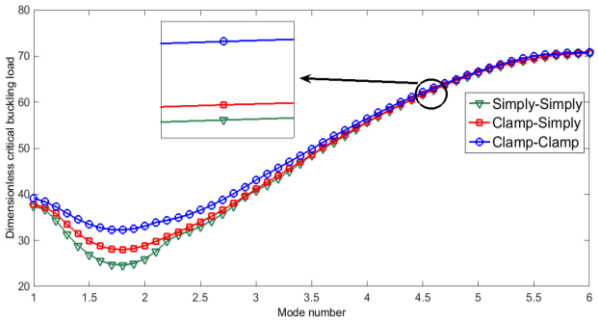


**Fig.8**
The variation of dimensionless critical buckling load versus the mode number of a cylindrical sandwich panel with different boundary conditions when $L$=1; $R$=$L$/3; $h$=0.1$R$; $h_c = h / 2$.

## 5 CONCLUSIONS

In this paper, the free vibration and buckling analysis of a cylindrical sandwich panel with an elastic core under various boundary conditions and subjected to various thermal and mechanical loadings was performed. The displacement field was described by the FSDT and the governing equations of motion were derived using the principle of minimum total potential energy. The temperature distribution in the cylindrical sandwich panel in the absence of a heat-generation source was obtained by solving the steady-state heat transfer equation. The accuracy of the presented model was verified with previous studies and with the results obtained by Navier analytical method. The GDQM was applied to discretize the equations of motion. The results indicated that some key parameters such as the length-to-radius ratio, circumferential wave numbers, thermal loadings, thickness ratio of core, and boundary conditions, play an important role on the buckling and vibrational response of the cylindrical sandwich panel.

## REFERENCES

[1] Lim C., Ma Y., Kitipornchai S., Wang C., Yuen R., 2003, Buckling of vertical cylindrical shells under combined end pressure and body force, *Journal of Engineering Mechanics* **129**: 876-884.
[2] Librescu L., Marzocca P., 2003, *Thermal Stresses*, Virginia Polytechnic Institute and State University, Blacksburg.
[3] Noor A. K., Burton W. S., 1992, Computational models for high-temperature multilayered composite plates and shells, *Applied Mechanics Reviews* **45**: 419-446.
[4] Lam K., Loy C., 1995, Effects of boundary conditions on frequencies of a multi-layered cylindrical shell, *Journal of Sound and vibration* **188**: 363-384.
[5] Li X., Chen Y., 2002, Transient dynamic response analysis of orthotropic circular cylindrical shell under external hydrostatic pressure, *Journal of Sound and Vibration* **257**: 967-976.
[6] Loy C., Lam K., 1999, Vibration of thick cylindrical shells on the basis of three-dimensional theory of elasticity, *Journal of Sound and Vibration* **226**: 719-737.
[7] Young P., 2000, Application of a three-dimensional shell theory to the free vibration of shells arbitrarily deep in one direction, *Journal of Sound and Vibration* **238**: 257-269.
[8] Shariyat M., 1997, Elastic, plastic, and creep buckling of imperfect cylinders under mechanical and thermal loading, *Journal of Pressure Vessel Technology* **119**: 27-36.
[9] Eslami M., Ziaii A., Ghorbanpour A., 1996, Thermoelastic buckling of thin cylindrical shells based on improved stability equations, *Journal of Thermal Stresses* **19**: 299-315.
[10] Radhamoman S., Enkataramana J., 1975,Thermal buckling of orthotropic cylindrical shells, *AIAA Journal* **13**: 397-399.
[11] Alibeigloo A., 2014, Three-dimensional thermo-elasticity solution of sandwich cylindrical panel with functionally graded core, *Composite Structures* **107**: 458-468.
[12] Thangaratnam R. K., Palaninathan R., Ramachandran J., 1990,Thermal buckling of laminated composite shells, *AIAA Journal* **28**: 859-860.
[13] Bert C., 1993, Buckling and post-buckling of composite plates and shells subjected to elevated temperature, *Journal of Applied Mechanics* **60**(2): 514-519.

[14] Mohammad-Abadi M., Daneshmehr A., 2015, Modified couple stress theory applied to dynamic analysis of composite laminated beams by considering different beam theories, *International Journal of Engineering Science* **87**: 83-102.
[15] Dumir P., Nath J., Kumari P., Kapuria S., 2008, Improved efficient zigzag and third order theories for circular cylindrical shells under thermal loading, *Journal of Thermal Stresses* **31**: 343-367.
[16] Kant T., Khare R., 1994, Finite element thermal stress analysis of composite laminates using a higher-order theory, *Journal of Thermal stresses* **17**: 229-255.
[17] Khdeir A., Rajab M., Reddy J., 1992, Thermal effects on the response of cross-ply laminated shallow shells, *International Journal of Solids and Structures* **29**: 653-667.
[18] Khare R. K., Kant T., Garg A. K., 2003, Closed-form thermo-mechanical solutions of higher-order theories of cross-ply laminated shallow shells, *Composite Structures* **59**: 313-340.
[19] Sheng G., Wang X., 2007, Effects of thermal loading on the buckling and vibration of ring-stiffened functionally graded shell, *Journal of Thermal Stresses* **30**: 1249-1267.
[20] Sheng G., Wang X., 2010, Thermoelastic vibration and buckling analysis of functionally graded piezoelectric cylindrical shells, *Applied Mathematical Modelling* **34**: 2630-2643.
[21] Shiau L.-C., Kuo S.-Y., 2004, Thermal postbuckling behavior of composite sandwich plates, *Journal of Engineering Mechanics* **130**: 1160-1167.
[22] Jeng-Shian C., 1990, FEM analysis of buckling and thermal buckling of antisymmetric angle-ply laminates according to transverse shear and normal deformable high order displacement theory, *Computers & Structures* **37**: 925-946.
[23] Rao K. M., 1985, Buckling analysis of anisotropic sandwich plates faced with fiber-reinforced plastics, *AIAA Journal* **23**: 1247-1253.
[24] Noor A. K., Starnes Jr J. H., Peters J. M., 1997, Curved sandwich panels subjected to temperature gradient and mechanical loads, *Journal of Aerospace Engineering* **10**: 143-161.
[25] Chang C.-C., 2012, Thermoelastic behavior of a simply supported sandwich panel under large temperature gradient and edge compression, *Journal of the Aerospace Sciences* **2012**: 480.
[26] Huang H., 2003, The initial post-buckling behavior of face-sheet delaminations in sandwich composites, *Journal of Applied Mechanics* **70**: 191-199.
[27] Huang H., Kardomateas G. A., 2002, Buckling and initial postbuckling behavior of sandwich beams including transverse shear, *AIAA Journal* **40**: 2331-2335.
[28] Frostig Y., Thomsen O. T., 2008, Non-linear thermal response of sandwich panels with a flexible core and temperature dependent mechanical properties, *Composites Part B: Engineering* **39**: 165-184.
[29] Khalili S., Mohammadi Y., 2012, Free vibration analysis of sandwich plates with functionally graded face sheets and temperature-dependent material properties: A new approach, *European Journal of Mechanics-A/Solids* **35**: 61-74.
[30] Leonenko D., Starovoitov E., 2016, Vibrations of cylindrical sandwich shells with elastic core under local loads, *International Applied Mechanics* **52**: 359-367.
[31] Malekzadeh F. K., Malek M. H., 2017, Free vibration and buckling analysis of sandwich panels with flexible cores using an improved higher order theory, *Journal of Solid Mechanics* **9**(1): 39-53.
[32] Jabbari M., Zamani N. M., Ghannad M., 2017, Stress analysis of rotating thick truncated conical shells with variable thickness under mechanical and thermal loads, *Journal of Solid Mechanics* **9**(1): 100-114.
[33] Saviz M., 2016, Coupled vibration of partially fluid-filled laminated composite cylindrical shells, *Journal of Solid Mechanics* **8**: 823-839.
[34] Golpayegani I. F., 2018, Calculation of natural frequencies of bi-layered rotating functionally graded cylindrical shells, *Journal of Solid Mechanics* **10**: 216-231.
[35] Saadatfar M., Aghaie K. M., 2015, On the magneto-thermo-elastic behavior of a functionally graded cylindrical shell with pyroelectric layers featuring interlaminar bonding imperfections rested in an elastic foundation, *Journal of Solid Mechanics* **7**(3): 344-363.
[36] Ghasemi A., Hajmohammad M., 2017, Evaluation of buckling and post buckling of variable thickness shell subjected to external hydrostatic pressure, *Journal of Solid Mechanics* **9**: 239-248.
[37] Hosseini-Hashemi S., Abaei A., Ilkhani M., 2015, Free vibrations of functionally graded viscoelastic cylindrical panel under various boundary conditions, *Composite Structures* **126**: 1-15.
[38] Thinh T. I., Nguyen M. C., Ninh D. G., 2014, Dynamic stiffness formulation for vibration analysis of thick composite plates resting on non-homogenous foundations, *Composite Structures* **108**: 684-695.
[39] Tauchert T. R., 1974, *Energy Principles in Structural Mechanics*, McGraw-Hill Companies.
[40] Reddy J. N., 2004, *Mechanics of Laminated Composite Plates and Shells: Theory and Analysis*, CRC Press.
[41] Ghadiri M., SafarPour H., 2017, Free vibration analysis of size-dependent functionally graded porous cylindrical microshells in thermal environment, *Journal of Thermal Stresses* **40**: 55-71.
[42] Bellman R., Casti J., 1971, Differential quadrature and long-term integration, *Journal of Mathematical Analysis and Applications* **34**: 235-238.
[43] Bellman R., Kashef B., Casti J., 1972, Differential quadrature: a technique for the rapid solution of nonlinear partial differential equations, *Journal of Computational Physics* **10**: 40-52.
[44] Shu C., 2012, *Differential Quadrature and its Application in Engineering*, Springer Science & Business Media.
[45] Shu C., Richards B. E., 1992, Application of generalized differential quadrature to solve two-dimensional incompressible Navier-Stokes equations, *International Journal for Numerical Methods in Fluids* **15**: 791-798.

[46] Loy C., Lam K., Shu C., 1997, Analysis of cylindrical shells using generalized differential quadrature, *Shock and Vibration* **4**: 193-198.
[47] Loy C., Lam K., Reddy J., 1999, Vibration of functionally graded cylindrical shells, *International Journal of Mechanical Sciences* **41**: 309-324.
[48] Matsunaga H., 2009, Free vibration and stability of functionally graded circular cylindrical shells according to a 2D higher-order deformation theory, *Composite Structures* **88**: 519-531.
[49] Rabani Bidgoli M., Saeed Karimi M., Ghorbanpour Arani A., 2016, Nonlinear vibration and instability analysis of functionally graded CNT-reinforced cylindrical shells conveying viscous fluid resting on orthotropic Pasternak medium, *Mechanics of Advanced Materials and Structures* **23**: 819-831.